Battery temperature aware equivalent consumption minimization strategy for mild hybrid electric vehicle powertrains

Battery temperature aware equivalent consumption minimization strategy for mild hybrid electric vehicle powertrains

Matteo Acquarone*,†, Pier Giuseppe Anselma*,‡, Federico Miretti*,†, Daniela Misul*,†
*CARS@PoliTo - Center for Automotive Research and Sustainable Mobility,
Politecnico di Torino, C.so Ferrucci 112, Torino, TO 10138, Italy
†Department of Energy "Galileo Ferraris" (DENERG),
Politecnico di Torino, Corso Duca degli Abruzzi 24, Torino, TO 10129, Italy
‡Department of Mechanical and Aerospace Engineering (DIMEAS),
Politecnico di Torino, Corso Duca degli Abruzzi 24, Torino, TO 10129, Italy
Email: federico.miretti@polito.it

***Abstract*—An energy management strategy for mild hybrids that prevents battery overheating is introduced in this digest. Energy management strategy design for mild hybrids requires particular care to prevent overheating of the battery pack as they typically do not have an active cooling system. To tackle this issue, we extend the well-known equivalent consumption minimization strategy approach to develop a real-time capable fuel-optimal controller that is sensitive to the battery's thermal dynamics and that can enforce constraints on its temperature. The rationale for our formulation is developed using Pontryagin's minimum principle from optimal control theory. The same principle is also used to design an off-line numerical procedure for the energy management strategy's calibration. The effectiveness of the procedure is corroborated by numerical experiments on two different drive cycles, whose results are also compared with the solution obtained with a dynamic programming algorithm. Several peculiar aspects of our solution procedure, such as the method used to incorporate state constraints and the approximate boundary value problem solution method using a particle swarm optimization algorithm, are also detailed and discussed. The proposed controller is computationally light-weight and can be readily extended to on-line control provided that a suitable co-state selection procedure is employed, based on the data collected by using our calibration method on a large number of driving missions.**

***Index Terms*—mild hybrid, hybrid electric, predictive, thermal management, passive cooling, battery**

I. Introduction

The market of mild hybrid electric vehicles (HEVs) is currently valued at 71.19 billion USD and it is forecast achieving a 17.45% annual growth rate over the next five years [1]. Effective energy management is a key requirement for enhancing the fuel economy of mild HEVs. In a mild HEV, the energy management strategy (EMS) is responsible for controlling the mechanical power split between the internal combustion engine (ICE) and the belt-starter generator (BSG).

EMSs for mild HEVs can be classified between off-line and on-line approaches depending on the future driving conditions being known a priori beforehand or not, respectively [2]. Obviously, only on-line EMSs are implementable on-board mild HEVs since knowing the profile of the vehicle speed over time for the entire drive cycle in advance is not possible. Several on-line EMSs for mild HEVs have been proposed in the literature, involving for example Pontryagin's minimum principle (PMP) [3], rule-based [4], and reinforcement learning [5].

Mild HEVs embed a 48V battery pack which is an important power component and requires dedicated management. For example, overheating the 48V battery pack needs to be prevented since it may lead to thermal runaway and accelerated aging [6]. This concern especially holds for mild HEVs since they typically use a passive cooling system. This means that the EMS provides compliance with the battery thermal limits by appropriately limiting its charge and discharge currents over time. At the same time, a significant use of the 48V battery pack is crucial to enable fuel saving in mild HEVs. Finding the right trade-off between fuel economy enhancement and preventing battery overheating is not trivial.

When developing the EMS for a mild HEV, several research works neglect the 48V battery pack temperature evolution over time in their vehicle modeling approach [3], [5]. Other research works model the battery temperature evolution over time, however they do not use this information as a feedback loop to the EMS of the electrified powertrain [7]. To the best of the authors' knowledge, improving the fuel economy effectiveness of the real-time EMS for mild HEVs while taking into account the evolution of the battery temperature over time is still an open research question.

Equivalent consumption minimization strategy (ECMS) is a well-known real-time near-optimal EMS for HEV powertrains [8]. In its traditional formulation, the instantaneous cost function which needs minimization in ECMS considers the fuel rate and the equivalent fuel consumption associated to the battery power weighted according to the value of an equivalence factor [9]. Zhou et al. assessed the impact of the value of equivalence factor on the battery temperature and aging entailed by an ECMS HEV controller [10]. In this work,

we apply Pontryagin's minimum principle to develop a version of the ECMS which includes a term related to the battery's temperature in the cost function. This allows optimizing the mild HEV powertrain control towards enhancing fuel economy while avoiding 48V battery overheating. Compared with a baseline ECMS formulation, the proposed battery temperature aware ECMS is demonstrated guaranteeing compliance with the battery thermal limits.

Recently, Maamria [11] presented a set of methods using the minimum principle to design an EMS taking the thermal dynamics of the engine and after-treatment systems into account. Our work focuses on the battery's thermal dynamics instead and is driven by a specific application, that is a mild hybrid without an active battery cooling system. Another notable difference with our work is that Maamria enforces state constraints on the battery state of charge (SOC) by adding a penalty term to the cost function (this is known as an interior point method). This method unfortunately has a major drawback of having to tune at least one penalty factor for each constraint, which becomes highly impractical as more constraints are added as we do in our work.

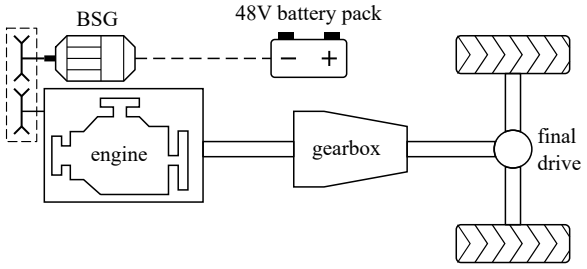

Fig. 1. p0 HEV architecture.

Finally, another difference of our method with respect to the minimum principle applications to the EMS design that can be found in the literature is that we do not attempt to find an exact solution to the associated boundary value problem but rather look for an approximate solution using a particle swarm optimization algorithm, as will be discussed later in the following section.

The rest of this paper is structured as follows: the p0 HEV simulation model (depicted in Figure 1) is briefly introduced first. The proposed battery temperature aware ECMS formulation is then presented, and a detailed procedure for its fuel-optimal calibration based on the minimum principle is described. Numerical results are then discussed, and conclusions are finally drawn.

II. Energy management strategy

The control strategy investigated in this paper works in a layered fashion. First, the gear number is set by a gear shift schedule as a function of the vehicle's speed. The optimization of the gear shift schedule is not treated in this work. Then, the energy management strategy sets the powerflow by controlling the e-machine torque-split factor, defined as the ratio between the e-machine's torque contribution at the gearbox input $T_{\mathrm{em,gb}}$ and the torque demand T_{d}, i.e. $\alpha = \frac{T_{\mathrm{em,gb}}}{T_{\mathrm{req}}}$.

The torque demand was evaluated as a function of the vehicle's speed v_{veh} and acceleration a_{veh} using a backward-facing quasi-static model [12]:

$$T_{\mathrm{d}} = \frac{F_{\mathrm{veh}}(v_{\mathrm{veh}}, a_{\mathrm{veh}}) r_{\mathrm{wh}}}{\tau_{\mathrm{fd}} \tau_{\mathrm{gb}}(\gamma)}, \tag{1}$$

where r_{wh} is the wheels' radius, τ_{fd} and τ_{gb} are the final drive and gearbox speed ratios, and γ is the gear number. The tractive effort F_{veh} was evaluated using a longitudinal vehicle model with a set of rolling resistance coefficients [13], [14]. Note that the vehicle speed and acceleration are defined by a vehicle driving mission; therefore, they are explicit functions of time and so is T_{d} (although we omit this in (1) for conciseness).

To derive a fuel-optimal energy management strategy, the presented EMS design problem was formulated as an optimal control problem and then solved with an indirect method [15]. In essence, indirect methods involve deriving necessary conditions of optimality using the minimum principle and then transcribing these into a *boundary value problem* (BVP) whose solution yields the optimal control trajectory as well as the optimal state and co-state trajectories. Compared to other approaches to EMS design such as dynamic programming, they are generally far less computationally expensive while still retaining high accuracy. However, this does not mean that their numerical solution is easy: BVPs of this kind require a good initial guess of the solution in order to converge [16].

The system state was defined by two state variables: the battery's state of charge σ and temperature T_{b}. This allows to formulate the charge-sustaining constraint that $\sigma(t_{\mathrm{f}}) = \sigma(t_0) = \sigma_0$ and the battery temperature constraint $T_{\mathrm{b}}(t) \leq T_{\mathrm{b,ub}}$, where $T_{\mathrm{b,ub}}$ is the maximum allowable temperature.

The battery's SOC dynamics was modeled using an internal resistance model:

$$\dot{\sigma} = \frac{i_{\mathrm{b}}}{Q_{\mathrm{b}}}, \tag{2}$$

$$i_{\mathrm{b}} = \frac{v_{\mathrm{oc}} - \sqrt{v_{\mathrm{oc}}^2 - 4 R_{\mathrm{eq}} P_{\mathrm{b}}}}{2 R_{\mathrm{eq}}}, \tag{3}$$

where i_{b}, v_{oc}, R_{eq} and Q_b are the battery current, open-circuit voltage, equivalent resistance and capacity. The open-circuit voltage and equivalent resistance were characterized as a function of both the battery state of charge and temperature. The battery power P_{b} does not depend on the state variables and is only a function of the control variable α and time (through the torque demand). Ultimately, because of the battery characteristics' dependence on the state variables, the current and the SOC dynamics are dependent on both states and the the torque-split factor α as well as time, i.e. $i_{\mathrm{b}} = i_{\mathrm{b}}(\sigma, T_{\mathrm{b}}, \alpha, t)$ and $\dot{\sigma} = \dot{\sigma}(\sigma, T_{\mathrm{b}}, \alpha, t)$.

The battery's thermal dynamics were modeled considering the heat generated due to the Joule losses and the convective heat transfer with the surrounding environment [17]–[19]:

$$\dot{T}_{\mathrm{b}} = \frac{1}{C_{\mathrm{b}}} \left(R_{\mathrm{eq}} i_{\mathrm{b}}^2 - h A_{\mathrm{b}} (T_{\mathrm{b}} - T_{\mathrm{env}}) \right), \tag{4}$$

where C_b is the battery's thermal capacity. Heat transfer to the environment was modeled as proportional to the temperature difference between the battery (T_b) and the surrounding air (T_env) via the heat exchange area A_b and a heat transfer coefficient h. Because of this as well as the dependence on the battery current, the battery's thermal dynamics depends on the state variables in addition to α and t, i.e. $\dot{T}_\mathrm{b} = \dot{T}_\mathrm{b}(\sigma, T_\mathrm{b}, \alpha, t)$.

The running cost was set as the fuel flow rate $\dot{m}_\mathrm{f}$, which was evaluated using a steady-state map as a function of the engine speed ω_eng and torque T_eng [14], [20], [21]. Therefore, it is ultimately a function of α and t.

In addition to the various control-dependent constraints that must be formulated to enforce feasibility of the powertrains components' operation (e.g. enforcing the limit torques of the engine and e-machine), we want to formulate state inequality constraints on the battery SOC and temperature, so that

$$\sigma \leq \sigma_\mathrm{ub}, \tag{5}$$

$$\sigma \geq \sigma_\mathrm{lb}, \tag{6}$$

$$T_\mathrm{b} \leq T_\mathrm{b,ub}, \tag{7}$$

where lb and ub define lower and upper bounds.

In order to incorporate these constraints in our necessary conditions for optimality, we follow the approach described in [15, Chapter 5.3] and we introduce an additional state variable η whose dynamics are defined by

$$\begin{aligned}\dot{\eta} = (\sigma - \sigma_\mathrm{ub})^2\, \mathbb{1}(\sigma - \sigma_\mathrm{ub}) + (\sigma_\mathrm{lb} - \sigma)^2\, \mathbb{1}(\sigma_\mathrm{lb} - \sigma) \\ + (T_\mathrm{b} - T_\mathrm{b,ub})^2\, \mathbb{1}(T_\mathrm{b} - T_\mathrm{b,ub})^1\end{aligned} \tag{8}$$

Note that, by definition, $\eta(t)$ is monotonically increasing in time and is strictly equal to zero only if the state constraints are never violated. In a way, this variable can be see as quantifying the constraints violation. Since our goal is to minimize this violation, we set $\eta(t_0) = 0$ and we require that the final state

$$\eta(t_\mathrm{f}) = \eta(t_0) + \int_{t_0}^{t_\mathrm{f}} \dot{\eta}(t)\, dt \tag{9}$$

is also equal to zero.

The Hamiltonian for this control system was therefore written as

$$\begin{aligned}H(\sigma, T_\mathrm{b}, \alpha, p_1, p_2, p_3, t) = \dot{m}_\mathrm{f}(\alpha, t) + p_1\, \dot{\sigma}(\sigma, T_\mathrm{b}, \alpha, t) \\ + p_2\, \dot{T}_\mathrm{b}(\sigma, T_\mathrm{b}, \alpha, t) + p_3\, \dot{\eta}(\sigma, T_\mathrm{b}, \alpha, t).\end{aligned} \tag{10}$$

For this problem, the principle states that if $\alpha(t)$ is the optimal control trajectory, then there must exist three co-state functions $p_1(t)$, $p_2(t)$ and $p_3(t)$ satisfying the adjoint equations

$$\dot{p}_1 = -\frac{\partial H}{\partial \sigma}, \tag{11}$$

$$\dot{p}_2 = -\frac{\partial H}{\partial T_\mathrm{b}}, \tag{12}$$

$$\dot{p}_3 = -\frac{\partial H}{\partial \eta} = 0, \tag{13}$$

[1]Here, $\mathbb{1}(\cdot)$ denotes the unit step function.

and such that $\alpha \in U(t)$ minimizes the Hamiltonian

$$H(\sigma, T_\mathrm{b}, \alpha, p_1, p_2, p_3, t), \tag{14}$$

where $U(t)$ defines the set of admissible controls and the Hamiltonian is defined by (10).

Furthermore, since the final temperature $T_\mathrm{b}(t_\mathrm{f})$ is free, the corresponding terminal co-state must satisfy the transversality condition:

$$p_2(t_\mathrm{f}) = \frac{\partial F(T_\mathrm{b}(t_\mathrm{f}))}{\partial T_\mathrm{b}} = 0, \tag{15}$$

where $F(T_\mathrm{b}(t_\mathrm{f}))$ is the terminal cost associated to the battery temperature. Since we did not want to associate a cost to the final battery temperature, this term was set to zero.

The adjoint equations (11)–(13) together with the state dynamics (2), (4) and (8) form a system of six differential equations. Correspondingly, six boundary conditions are provided by the initial and terminal states together with the transversality condition (15):

$$\sigma(t_0) = \sigma_0, \tag{16}$$

$$T_\mathrm{b}(t_0) = T_\mathrm{env}, \tag{17}$$

$$\eta(t_0) = 0, \tag{18}$$

$$\sigma(t_\mathrm{f}) = \sigma_0, \tag{19}$$

$$p_2(t_\mathrm{f}) = 0, \tag{20}$$

$$\eta(t_\mathrm{f}) = 0. \tag{21}$$

Together, these equations coupled with the Hamiltonian minimization and these boundary conditions form a BVP problem, as we previously mentioned. To solve this problem, the shooting method was employed. In indirect shooting, an initial guess is generated for all the boundary conditions at the left endpoint t_0. Then, the initial value problem composed by the differential equations coupled to this set of initial conditions is solved by numeric integration. In particular, we used a forward Euler integration scheme, and we obtained the partial derivatives in (11)–(13) using finite differences. The difference between the resulting boundary conditions at t_f and those imposed in the BVP is used to update the initial guess and the process is repeated.

The same procedure can also be formulated in terms of an optimization problem, where the optimization variables are the initial values of the co-states $p_1(t_0)$, $p_2(t_0)$ and $p_3(t_0)$ and the objective function is the difference between the corresponding $\sigma(t_\mathrm{f})$, $p_2(t_\mathrm{f})$ and $\eta(t_\mathrm{f})$ and those set by the boundary conditions (19)–(21).

This allowed us to use a particle swarm optimization (PSO) algorithm to calibrate the initial co-states. The reason we used a PSO algorithm to solve the BVP is that it proved to be quite robust with respect to a poor first guess. We attribute this to the fact that PSO is a derivative-free algorithm, hence it is less sensible to the strong lack of smoothness in the problem. This lack of smoothness is ultimately caused by the presence of non-continuously differentiable functions such as linear interpolants in the vehicle model, which are used to model e.g. the fuel consumption as is typical in quasi-static HEV powertrain models.

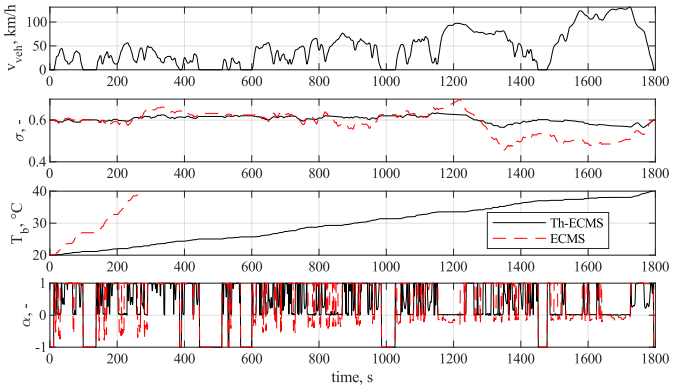

Fig. 2. Simulation profiles with a regular ECMS and the proposed formulation. The ECMS formulation proposed in this digest is labeled as *Th-ECMS*, while the regular implementation is denoted simply as ECMS.

Nonetheless, a proper derivative-based BVP solver would be likely be more computationally efficient, although this would come at the cost of increased modeling effort. A systematic comparison of these two different approaches would be an interesting topic but is out of the scope of this paper.

The objective function of the PSO solver was defined as a scalarized objective:

$$J(p(t_0)) = \frac{|\sigma(t_f) - \sigma_0|}{\bar{\sigma}} + \frac{|p_2(t_f)|}{\bar{p_2}} + \frac{\eta(t_f)}{\bar{\eta}} \qquad (22)$$

where $\bar{\sigma}$, $\bar{p_2}$ and $\bar{\eta}$ are normalization factors.

One thing that should be noted is that altough the PSO algorithm is able to reduce (22) to a very small quantity, it is never able to reduce it to exactly zero. This is also due to the many other approximations in the optimization process, such as the numerical integration error and the approximation of the adjoint equations by finite differences. Indeed, this reflects the fact that we are obtaining an approximate solution to the exact optimality conditions, as is typical of all indirect methods.

III. Results and Discussion

The procedure described in the previous section was implemented in MATLAB and tested on a number of driving cycles. Here, we report results for the WLTP (Worldwide Harmonised Light vehicles Test Procedure) and UDDS (Urban Dynamometer Driving Schedule) cycles. For each simulation, the parameters $p_1(t_0)$, $p_2(t_0)$ and $p_3(t_0)$ where calibrated using the PSO algorithm as described in the previous section in order to minimize fuel consumption while keeping the battery temperature below 40 °C, with an environment temperature of 20 °C. For the purpose of the Hamiltonian minimization, the torque-split factor α was discretized with a uniformly spaced grid of 121 values ranging from -1 to 1.

The effectiveness of the proposed implementation is shown in Figure 2. The Th-ECMS produces a solution hitting the constraints with great accuracy whereas a regular ECMS implementation violates the battery temperature constraint, making a larger use of the battery to maximize fuel economy and producing higher currents as a consequence. This is also clearly visible from the deeper charging and discharging observable from the SOC profiles. Furthermore, the regular ECMS produced a fuel economy of 6.46 l/100km while the Th-ECMS 6.67 l/100km. Since both are fuel-optimal, with the only difference being in the introduction of the battery temperature constraint, the gap between the two can be seen as the minimum gap that can be attained without introducing an active cooling system while keeping the battery under 40 °C, acting on the EMS design only.

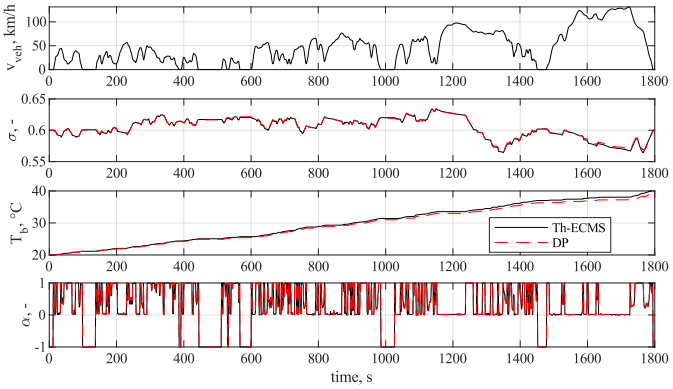

Fig. 3. Comparison of the Th-ECMS and the solution obtained with dynamic programming on the WLTP cycle.

As we mentioned in the previous section, due to a number of reasons related to the numerical solution of the BVP formulated with the minimum principle, we are obtaining an approximate solution to the necessary conditions of optimality. Moreover, the fact that these conditions are necessary but not sufficient does not guarantee global optimality but only local optimality. To assess the optimality of our method, we compared simulation results with the solution obtained using dynamic programming (DP). While DP uses its own approximations to obtain a solution, it is based on both necessary and sufficient conditions of optimality and is therefore often used as a benchmark.

For our simulations, we used a dedicated MATLAB toolbox called DynaProg [22]. The control variable α was discretized with a uniformly spaced grid of 121 values ranging from -1 to 1 (as for the ECMS). For the purpose of the value function update and evaluation, the state variables (the battery SOC and temperature) were discretized with uniformly spaced grids of 801 values ranging from 0.4 to 0.8 and 212 values ranging from 20 °C to 41 °C.

As reported in Table I, the Th-ECMS comes very close to dynamic programming in terms of fuel economy. In both the WLTP and UDDS, the difference is below 0.6 %. The fact that the Th-ECMS produces a slightly lower fuel economy can be explained by inspecting the simulation results shown in Figures 3 and 4. While the control and state profiles match quite well overall, there is a small but notable difference in the maximum temperatures reached. While the Th-ECMS reaches maximum temperatures of 40.3 °C and 40.2 °C on the UDDS and WLTP cycles respectively, dynamic programming only

reaches 39.6 °C and 39.2 °C.

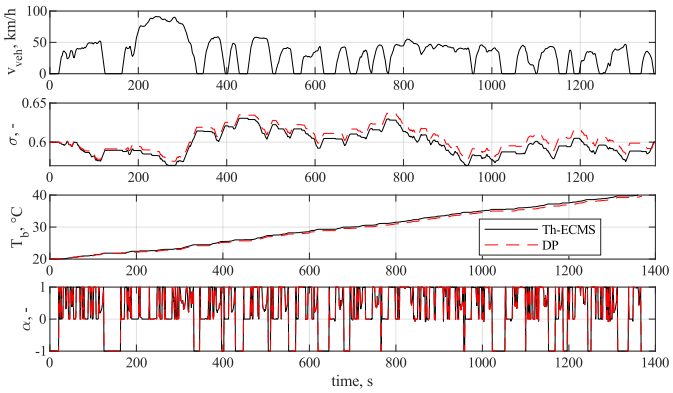

Fig. 4. Comparison of the Th-ECMS and the solution obtained with dynamic programming on the UDDS cycle.

This is due to the difference in the way the two algorithms handle state constraints. The dynamic programming algorithm enforces the state constraint as a hard constraint; moreover, the inherent characteristics of the value function approximation scheme tend to artificially penalize operating close[2] to the constraint boundary. On the other hand, the formulation of the minimum principle employed in this work to develop the Th-ECMS treats the state constraints as something similar to a soft constraint, where violations are strongly penalized by the requirement that the additional state $\eta(t)$ remains zero for all t.

TABLE I
FUEL ECONOMY OF THE PROPOSED TH-ECMS COMPARED TO THE DYNAMIC PROGRAMMING BENCHMARK.

Driving cycle	Fuel economy, l/(100 km)		Difference
	Th-ECMS	DP	
UDDS	5.79	5.83	0.6 %
WLTP	6.67	6.70	0.4 %

IV. CONCLUSIONS

In this paper, we described an EMS design approach that keeps the battery temperature under control suitable for 48V mild HEVs. The fact that we obtain the torque split-factor α by minimizing the Hamiltonian (10) essentially leads to an extension of the original ECMS approach with an additional term penalizing the battery temperature increase. In this sense, $p_2(t)$ can be seen as a time-varying equivalence factor for the battery heat power. While the methodology in this paper can be used to calibrate this parameter in an off-line design procedure, the approach could be used on-line if a suitable online co-state selection technique was adopted (see e.g. [16] and [23]). This research topic represents the first and most important development area of the present work.

[2]The meaning of *close* here depends on the state grids' discretization.

The inclusion of the battery temperature constraint in the formulation of the minimum principle was done with an approach that, when considering the approximate nature of the solution obtained to the resulting BVP, effectively behaves like a soft constraint, with the final state $\eta(t_f)$ being a measure of the extent of the constraint violation in both magnitude and violation time. To make it as close as possible to a hard constraint, we aimed at bringing this value to zero when solving the BVP. An alternative approach that is enabled by this technique would be to leave $\eta(t_f)$ free and to formulate a terminal cost $F(\eta(t_f))$ instead, which would replace the boundary condition (21) with an additional transversality condition. This terminal cost could be formulated based on techno-economical considerations to reflect the amount of damage (in terms of lifetime reduction) taken by the battery as a result of overheating and/or crossing the SOC bounds.

Finally, another important area of investigation which may further improve the methods presented in this paper would be to carry out a systematic comparison of the PSO solver used in this paper with more standard BVP solvers. This may in turn enable the development of a robust and computationally fast technique which combines the advantages of both. For example, since PSO is naturally well-suited for multi-objective optimization, it could be used to generate a set of first guesses which are close enough to enforcing the right boundary conditions (at t_f) and then using a computationally fast and accurate state-of-the-art BVP solver to obtain the proper solution.

REFERENCES

[1] Mordor Intelligence, "Mild hybrid vehicles market - growth, trends, covid-19 impact, and forecasts (2022 - 2027)," Tech. Rep., feb 2022.

[2] E. Silvas, T. Hofman, N. Murgovski, P. Etman, and M. Steinbuch, "Review of optimization strategies for system-level design in hybrid electric vehicles," *IEEE Transactions on Vehicular Technology*, pp. 1–1, 2016.

[3] L. Thibault, A. Sciarretta, and P. Degeilh, "Reduction of pollutant emissions of diesel mild hybrid vehicles with an innovative energy management strategy," in *2017 IEEE Intelligent Vehicles Symposium (IV)*. IEEE, jun 2017.

[4] R. M. Bagwe, A. Byerly, E. C. dos Santos, and Ben-Miled, "Adaptive rule-based energy management strategy for a parallel HEV," *Energies*, vol. 12, no. 23, p. 4472, nov 2019.

[5] B. Xu, F. Malmir, D. Rathod, and Z. Filipi, "Real-time reinforcement learning optimized energy management for a 48v mild hybrid electric vehicle," in *SAE Technical Paper Series*. SAE International, apr 2019.

[6] C. Yu, G. Ji, C. Zhang, J. Abbott, M. Xu, P. Ramaekers, and J. Lu, "Cost-efficient thermal management for a 48v li-ion battery in a mild hybrid electric vehicle," *Automotive Innovation*, vol. 1, no. 4, pp. 320–330, nov 2018.

[7] S. Lee, J. Cherry, M. Safoutin, J. McDonald, and M. Olechiw, "Modeling and validation of 48v mild hybrid lithium-ion battery pack," *SAE International Journal of Alternative Powertrains*, vol. 7, no. 3, pp. 273–287, apr 2018.

[8] A. Sciarretta, L. Serrao, P. Dewangan, P. Tona, E. Bergshoeff, C. Bordons, L. Charmpa, P. Elbert, L. Eriksson, T. Hofman, M. Hubacher, P. Isenegger, F. Lacandia, A. Laveau, H. Li, D. Marcos, T. Nüesch, S. Onori, P. Pisu, J. Rios, E. Silvas, M. Sivertsson, L. Tribioli, A.-J. van der Hoeven, and M. Wu, "A control benchmark on the energy management of a plug-in hybrid electric vehicle," *Control Engineering Practice*, vol. 29, pp. 287–298, aug 2014.

[9] G. Paganelli, T. M. Guerra, S. Delprat, J.-J. Santin, M. Delhom, and E. Combes, "Simulation and assessment of power control strategies for a parallel hybrid car," *Proceedings of the Institution of Mechanical Engineers, Part D: Journal of Automobile Engineering*, vol. 214, no. 7, pp. 705–717, jul 2000.

[10] B. Zhou, A. Rezaei, and J. Burl, "Effect of battery temperature on fuel economy and battery aging when using the equivalent consumption minimization strategy for hybrid electric vehicles," in *SAE Technical Paper Series*. SAE International, apr 2020.
[11] D. Maamria, "Dynamic optimization in multi-states systems for automobile energy efficiency," Ph.D. dissertation, Ecole Nationale Supérieure des Mines de Paris, 2015.
[12] L. Guzzella and A. Sciarretta, *Vehicle Propulsion Systems*. Springer Berlin Heidelberg, 2013.
[13] C. E. Chapin, "Road load measurement and dynamometer simulation using coastdown techniques," in *SAE Technical Paper Series*. SAE International, jun 1981.
[14] M. Ehsani, Y. Gao, S. E. Gay, and A. Emadi, *Modern Electric, Hybrid Electric, and Fuel Cell Vehicles*. CRC Press, dec 2004.
[15] D. E. Kirk, *Optimal control theory; An introduction*. Englewood Cliffs, N.J: Prentice-Hall, 1970.
[16] T. J. Böhme and B. Frank, *Hybrid Systems, Optimal Control and Hybrid Vehicles*. Springer International Publishing, 2017.
[17] C. Forgez, D. V. Do, G. Friedrich, M. Morcrette, and C. Delacourt, "Thermal modeling of a cylindrical LiFePO4/graphite lithium-ion battery," *Journal of Power Sources*, vol. 195, no. 9, pp. 2961–2968, may 2010.
[18] T. Huria, M. Ceraolo, J. Gazzarri, and R. Jackey, "High fidelity electrical model with thermal dependence for characterization and simulation of high power lithium battery cells," in *2012 IEEE International Electric Vehicle Conference*. IEEE, mar 2012.
[19] L. Saw, Y. Ye, and A. Tay, "Electro-thermal characterization of lithium iron phosphate cell with equivalent circuit modeling," *Energy Conversion and Management*, vol. 87, pp. 367–377, nov 2014.
[20] J. D. Bishop, M. E. Stettler, N. Molden, and A. M. Boies, "Engine maps of fuel use and emissions from transient driving cycles," *Applied Energy*, vol. 183, pp. 202–217, dec 2016.
[21] J. Heywood, *Internal combustion engine fundamentals*. McGraw-Hill Education, 2018.
[22] F. Miretti, D. Misul, and E. Spessa, "DynaProg: Deterministic dynamic programming solver for finite horizon multi-stage decision problems," *SoftwareX*, vol. 14, p. 100690, jun 2021.
[23] B. Jager, *Optimal Control of Hybrid Vehicles*. Springer London, 2013.